

THE MICROSTRUCTURE OF VERMICULAR GLAUCONY

SIMON G. McMILLAN

Department of Geology, University of Otago
P.O. Box 56, Dunedin, New Zealand

Abstract—Vermicular glaucony grains observed by transmission electron microscopy (TEM) show three irregularly alternating zones. Zone A has a high degree of linear orientation, no void space, and relatively defect-free lattice-fringe images. Zone B has an amalgamated bundle texture with a sub-parallel, linear orientation of bundles to each other and to zone A. Zone B has little or no void space, and lattice images appear to be a combination of those typical of zone C with minor amounts of modified zone A forms. Zone C has a randomly oriented, curved, and circular or semicircular bundle texture. In addition, zone C has much void space and curvilinear and linear lattice-fringe images with numerous defects, including edge dislocations. Such morphologic and crystallographic characteristics indicate that zones B and C probably comprise the glauconitic minerals of the vermicular glaucony grains, and that zone A comprises non-glauconitic micaceous minerals of higher structural order. Zone B is sharply demarcated from zone A, but B zone bundle textures merge gradationally to those of zone C. These spatial relationships suggest that zone B forms first on the surface of zone A. Sub-parallel orientation in the B zone could be produced by initial confinement between adjacent A zones. Once constraints change or are removed, the randomly oriented, curved, and semicircular or circular bundles of zone C develop.

Key Words—Transmission electron microscopy, Vermicular glaucony.

INTRODUCTION

The term glaucony was formally introduced by Odin (1988) as a facies name to describe green marine pigments comprising 2:1 layer dioctahedral glauconitic minerals such as interlayered glauconite-smectite and the 10 Å mineral glauconite. Glaucony displays two habits: a film habit such as occurs on hardground surfaces, and a granular habit (Odin 1988). Vermicular glaucony grains (also called vermiform, caterpillar, concertina, or accordion grains) are a morphological variety of granular glaucony characterized by curved, twisted, or elongate cylindrical shapes and an external accordion-like structure of packets or books stacked along the prominent elongation direction.

The replacement and transformation of detrital biotite was proposed as a mechanism for the development of “glauconite” by Galliher (1935). An intermediate stage of this development was the formation of an accordion-like morphology (p. 1538 in Galliher, 1935). Using observations by Galliher and others, other authors, notably Burst (1958a, 1958b), developed the transformation hypothesis to account for the general formation of glauconite. Tapper and Fanning (1968) found no crystallographic difference in X-ray diffractograms of glauconite pellets displaying lobate and vermiform morphologies. This suggested that higher order micaceous minerals such as biotite or muscovite were not present within the vermiform glauconite observed by these authors. Tapper and Fanning (1968) concluded that, although such a finding did not substantiate Galliher's theory of a derivation from biotite, it did not discount the possibility of a derivation from some form of mica: All the mica could have been converted

to glauconite. They suggested alternative origins for the development of their “vermiform pellets.” These included formation from solution, which they considered unlikely, or via a recrystallization process. An alternative theory to the transformation hypothesis for the development of vermicular glaucony was proposed by Odin (1972) and enlarged by Odin and Matter (1981) and Odin (1988). It involved the neoformation of glauconitic minerals between, and their subsequent expansion of, the platy sheets of detritally derived biotite and muscovite. These authors noted the presence of unaltered or slightly altered mica within their accordion-like grains even when the evolution to a vermicular glaucony grain is essentially complete (Odin, 1988).

This paper investigates the microstructure of vermicular glaucony grains, which have a well-developed micaceous texture in petrographic thin section, as observed by transmission electron microscopy (TEM). It seeks to confirm which of the above theories is the most suitable for describing the mechanism of formation of vermicular glaucony.

EXPERIMENTAL METHODS

Samples

Samples containing vermicular glaucony were taken from the Eocene (Upper Ypresian-Lower Lutetian) part of the Abbotsford Formation (McMillan, 1993) at Boulder Hill, near Dunedin, New Zealand (Figure 1). These are homotaxial formations (Carter, 1988) deposited over a passively subsiding schist and metasedimentary basement during the late Cretaceous to mid-

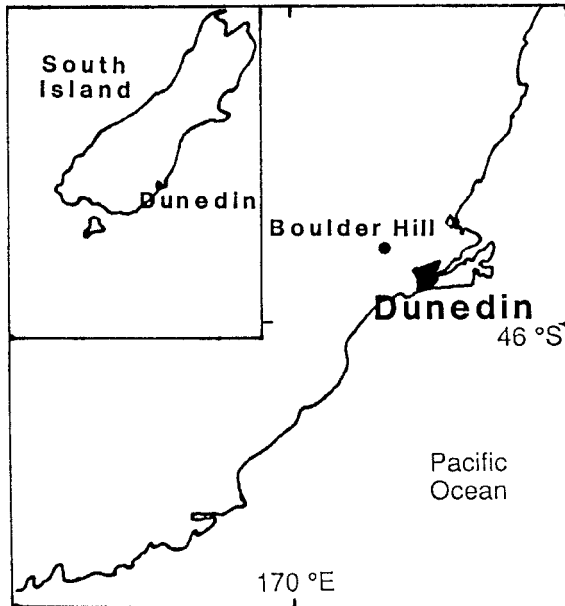


Figure 1. Location map of study area.

Tertiary (Oligocene) transgression of New Zealand (Carter and Norris, 1976; Norris *et al.*, 1978).

The external and internal morphology of the same vermicular glaucony grains described here have been documented in detail elsewhere (McMillan, 1993). External features include ridges, grooves, striations, and transverse partings separating green micaceous packets. Viewed with the petrographic microscope, vermicular glaucony grains exhibit a distinctive internal texture dominated by a cleavage oriented at right angles to their elongation direction (ED) (Figure 2). It was across this variously oriented cleavage that TEM images were taken.

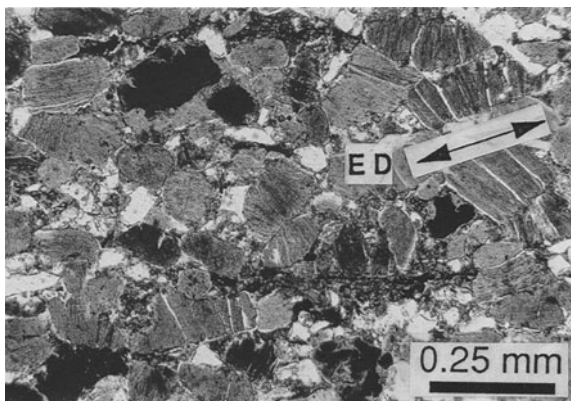


Figure 2. Photomicrograph of a greensand (>50% glaucony), dominated by vermicular glaucony grains with characteristic cleavage at right angles to the prominent elongation direction. Opaque grains are goethite.

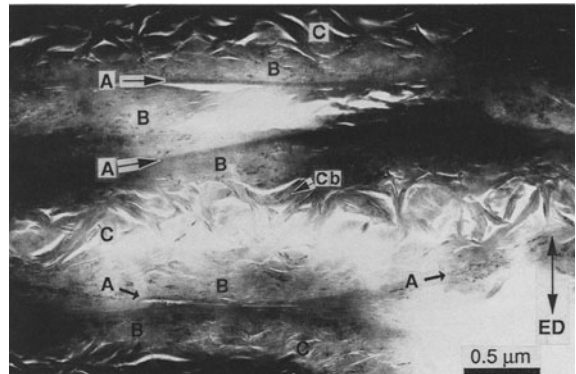


Figure 3. Low-resolution TEM image of alternating texture in vermicular glaucony. Three thin, curvilinear A zones are present from left to right. These are separated by randomly oriented bundles (Cb) of the C zone (C) with much void space and B zones with little or no void space and subparallel texture to the A zone. The approximate elongation direction (ED) of the vermicular glaucony grain is indicated.

Methods

Samples were prepared by ion-beam thinning of whole sediment wafers, following slight modification of the procedure of Phakey *et al.* (1972). Polished thin sections of epoxy-impregnated whole sediment, left at a thickness of approximately 20–30 μm , were mounted with an alcohol soluble resin on a glass slide. Areas were selected for analysis and copper mesh grids glued directly on the sediment slice. The sediment wafer with attached grids was removed from the glass slide by immersion in alcohol. Grids with attached sediment were trimmed from the wafer; strengthened by attachment of a single hole, aperture copper grid to the other

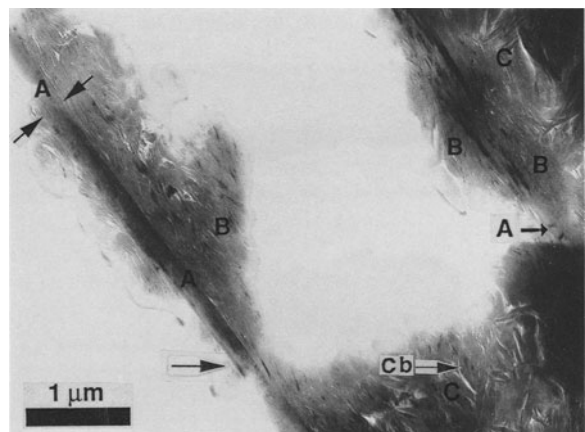


Figure 4. Low-resolution TEM image of A, B, and C zones within the alternating zonal texture in vermicular glaucony. Two A zones (between opposing arrows at top left and thin zone at far right) are separated by B and C zones. ED coincides with the line of the opposing arrow set and C zone bundles (Cb) are indicated. The arrow at bottom left indicates the area from which Figure 6a was taken.

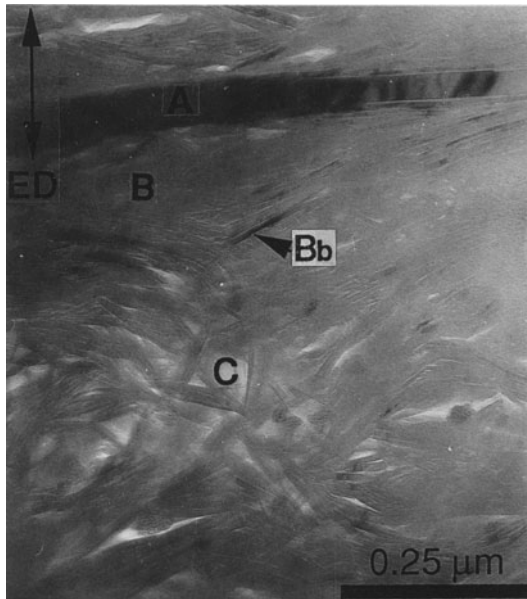


Figure 5. Low-resolution TEM image of A, B, and C zones with characteristic textures and closer view of zonal contacts. Contact of zone A with B is sharp and well defined, but zone B is gradational to zone C. Zone B bundles (Bb) have a sub-parallel orientation to zone A. The ED direction is indicated.

side; and mounted in the ion-beam thinner. The double-sided argon gun was oriented at 15° to the rotating specimen, and the accelerating voltage was kept between 4 to 5 kV. Thinning times varied between 3.5 and 4.5 hr. After applying a thin carbon layer, the thinnest areas of the sample next to perforations were used for viewing. All samples were viewed on a Phillips EM 410 at 100 kV. Both low- and high-resolution structures were obtained between 10 K to 240 K magnification. All micrographs were recorded using bright field illumination, and one-dimensional lattice images were obtained in the underfocus condition. Tilting was not applied due to potential electron beam damage of the specimen. Instrument constraints meant that chemical and SAD data were not obtained during the TEM investigations. Thus, the exact spacings of lattice fringe images were not ascertained.

RESULTS

Microstructure observations in vermicular glaucy

Vermicular glaucy grains exhibit a characteristic internal texture of three alternating zones: A, B, and C (Figure 3). These zones repeat, in the sequence A-B-C-B-A-B, etc., in a direction coincident with the ED of the vermicular glaucy grains (Figure 2). Commonly, the repeating distance is irregular but usually within the order of 0.5 to 6.0 μm for consecutive A zones. The repetition sequence of A zones is difficult to discern where an A zone is particularly thin or successively splayed (Figure 4). In such cases, only a B

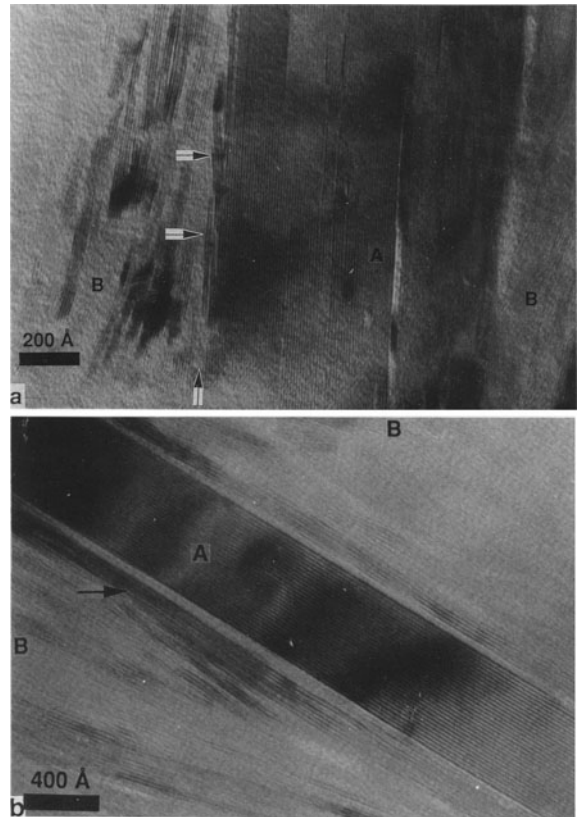


Figure 6. High-resolution TEM images of lattice fringes typical of the A zone: a) This micrograph was obtained from the area arrowed at bottom left in Figure 4. Lattice images of the A zone are straight, well-defined and can be traced for a distance of at least 3 μm along the length of the zone. The two horizontal arrows highlight areas where the A zone lattices are separated from the thicker A zone parent. In both cases, this occurs near edge dislocations (to the immediate right of both arrow points) in the A zone. The vertical arrow demarcates the boundary of the A and B zones. b) This micrograph was obtained from the A zone at top right in Figure 5. Straight well-defined lattices characterize the A zone. A group of less well-defined lattices (arrowed at upper left) are attached to the main A zone at top left.

zone may be clearly recognizable, and careful analysis of the micrograph may be required to identify the presence of the A zone morphology.

The A zone is characterized by strongly linear orientations (Figures 4 and 5). Thicknesses vary between 0.03 μm to 1 μm along individual and successive A zones. One-dimensional lattice-fringe images from this zone (Figure 6) are typically straight, well-defined, and relatively defect-free. The A zone lattice images can usually be differentiated from those of the B and C zones by the much greater distance along which they persist. For example, lattice images of the A zone in Figure 4 (bottom left) can be traced for distances of at least 3 μm . In contrast, lattice images in the C zone usually disappear over distances greater than 0.08 μm .

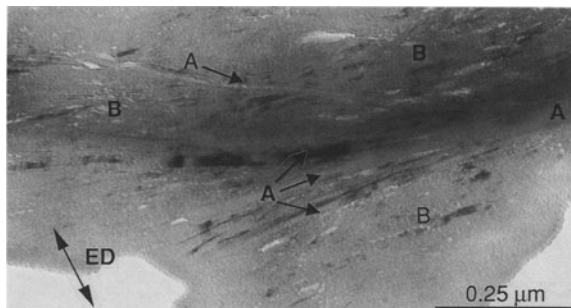


Figure 7. Low-resolution TEM image of splaying of a parent A zone. Zone B minerals surround, and are similarly oriented, to four zone A stringers. This image was collected within, rather than from the edge of, a vermicular glaucony grain.

Where A zones are thin, less than about $0.08 \mu\text{m}$ (Figure 3), or splayed (Figure 7), they may become curved with less strongly linear orientation. In these cases, A zone lattice images can also disappear over distances similar to those of zone C (Figure 8). The contact between zone A and B is a sharp linear line (Figure 5), but may become irregular where A zones become separated and splayed (Figure 7). The lattice images also exhibit mottled contrast bands over greater distances than the lattice images obtained from the C zone.

Zone B is characterized by a bundle texture with minor void space, where bundles have a sub-parallel or low-angle relationship with zone A and to each other (Figure 5). The B zone was always found closest to the A zone, but it can be poorly developed giving the appearance of C zones juxtaposed next to A zones (Figure 3). Thicknesses of the B zones are variable along the length of surrounding A zones, but are commonly between 0.2 to $5.0 \mu\text{m}$. Lattice-fringe images consist of some images like those in the A zone, but most are similar to those in the C zone (Figure 9). In general,

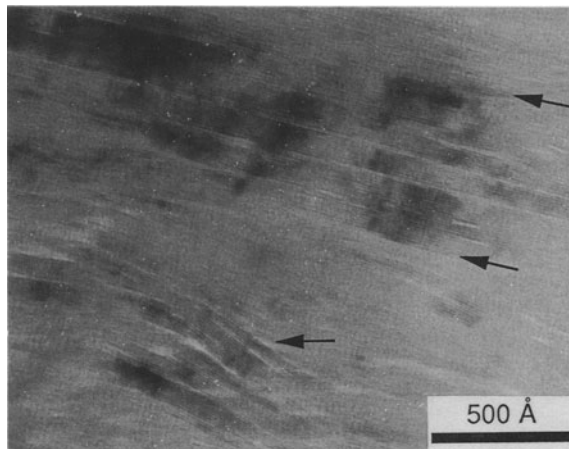


Figure 9. High-resolution TEM image of lattice fringes in the B zone. The morphology of the lattice images between the two arrows at right is similar to those of zone A. However, the curved, more poorly oriented lattices (arrowed at middle) are more likely those of the C zone.

lattice images were more easily obtained and present in greater number from this zone than from zone C.

Zone C is characterized by bundles with curved, randomly oriented, semicircular or circular textures with considerable void space (Figures 4, 5, and 10). Thicknesses are again variable, but commonly values are between 0.5 and $5.0 \mu\text{m}$. The contact with zone B is gradational, with bundle textures in zone B becoming increasingly curved into the C zone. Lattice fringe images exhibit a minor or patchy development of image mottling; frequent edge dislocations; and undulating, low-amplitude curved, wavy, or linear morphologies (Figure 11). Lattice images are arranged in crystallite bundles about 100 – 300 Å thick, with low-angle, parallel, and curved crystallite junctions to each other. As

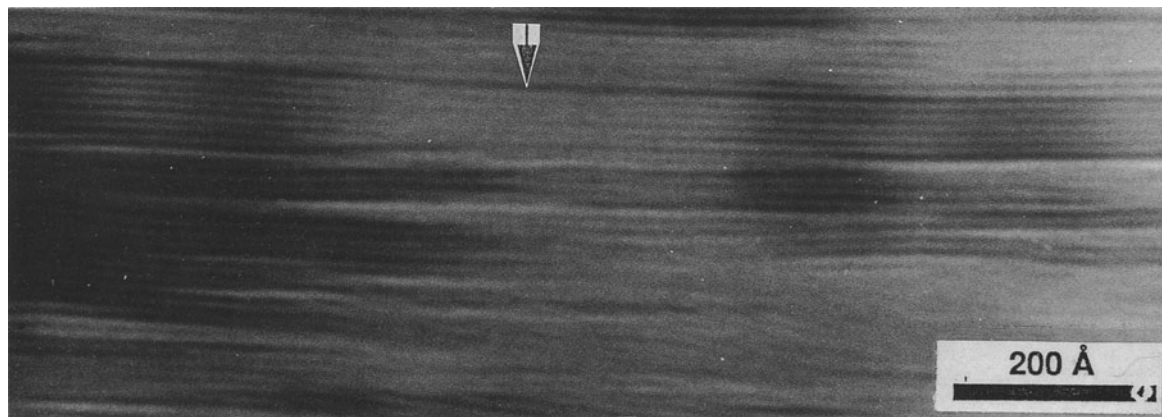


Figure 8. High-resolution TEM image of undulose A zones separated from their thicker parent in a splayed area similar to that in Figure 7. The lattice images of the A zone are discontinuous or absent in the middle of the micrograph (arrowed), but they are continuous on either side.

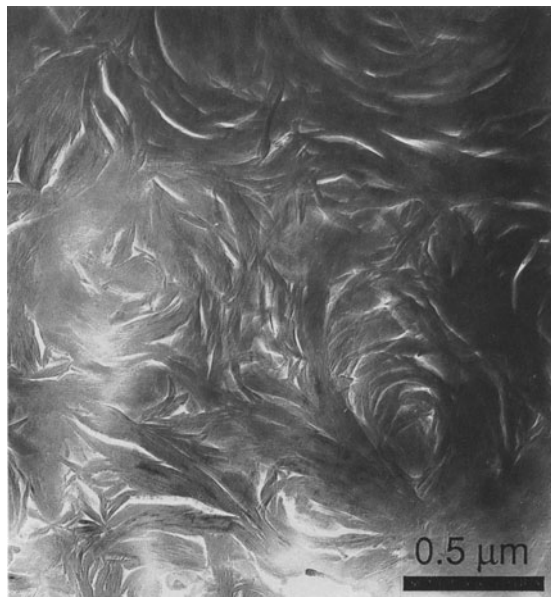


Figure 10. Low-resolution TEM image of semicircular and circular bundles observed in some C zones (areas at top and bottom right).

noted above, lattice images are lost over relatively small distances compared with those of the A zone.

DISCUSSION

Interpretation

The contacts and microstructure exhibited by the three zones yield clues to both the origin of zonation and to the formation of vermicular glaucy. The pronounced linearity displayed by the A zones and the presence of lattice-fringe images that are straight, well-defined, relatively defect-free, and that persist for distances at least up to 3 μm characterize more unidirectional orientation and more highly ordered structures than those of the C zone. The form of such lattice images is similar to those observed for biotite by Banfield and Eggleton (1988); for some more highly ordered illite crystals and illite/muscovite crystals in slate by Lee *et al.* (1985); for phengitic mica in slate by Ireland *et al.* (1983); and for sericite and pyrophyllite in hydrothermal vein deposits by Page (1980). The morphological features of the A zones are unlike known TEM data on glauconite grains (see C zone below).

The identity of the mineral phase(s) comprising the A zone is suggested to be that of phyllosilicate(s) derived from preexisting basement rocks formed at the pressures and temperatures necessary to produce the relatively high structural orders found. In support of this interpretation, some biotite and muscovite flakes are present within the whole sediment in what appear to be various stages of glaucy (Figure 13). The biotite and muscovite parts of these flakes, identified

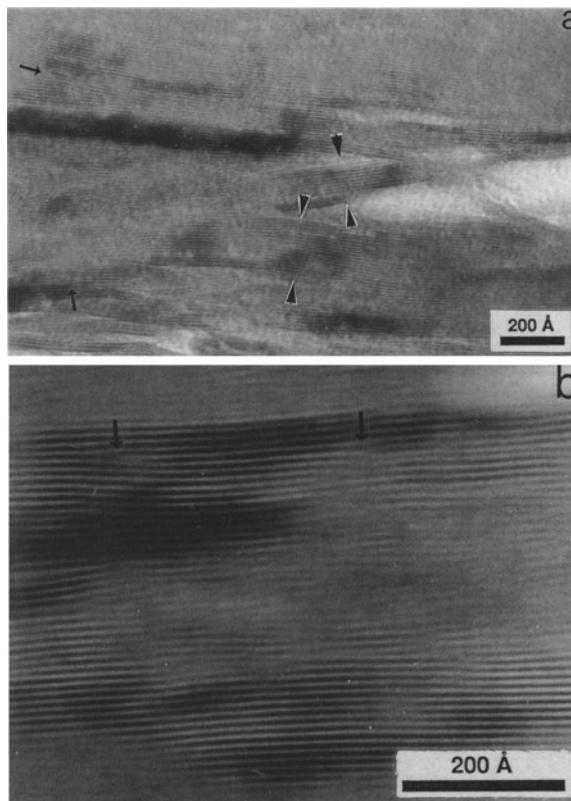


Figure 11. High-resolution TEM image of lattice fringes typical of the C zone with curved, linear, or wavy form: a) 100–300 \AA bundles of lattices (opposing sets of arrows at center) terminate with low-angle junction against other bundles (example arrowed at upper left), edge dislocation arrowed at bottom left; b) Wavy discontinuous form and numerous edge dislocations (arrowed).

by standard optical properties such as form, pleochroism, and higher-order birefringence, are sometimes interleaved with, or exhibit fan-like expansion textures coincident with, development of green randomly oriented microlites between the mica sheets (Figure 13). Biotite, chlorite, and muscovite substrates could have been readily provided from the nearby Otago Schist basement rocks (Brown, 1963; Wood, 1968) throughout the late Cretaceous-Eocene interval (Carter and Norris, 1976; Norris *et al.*, 1978).

The texture of the B zone is similar to that of the C zone in that both exhibit a bundle texture not found in the A zone. However, the subparallel linearity of the bundle texture with the A zone is different and is interpreted as the result of a confining force on bundle development that is not apparent as the C zone textures form. The gradual change in bundle orientation from the B to the C zone suggests a similar mineral identity.

The TEM bundle textures of zone C are similar to the textures exhibited by glaucy grains that show petrographic textures of randomly oriented microlites (Figure 12; Ireland *et al.*, 1983, Figure 1), with con-

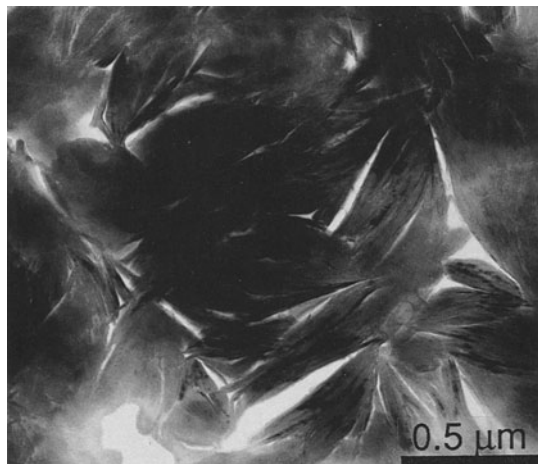


Figure 12. Low-resolution TEM image of unoriented bundles in non-vermicular glaucony grains that exhibit a texture of randomly oriented microlites under the petrographic microscope.

siderable void space visible in both. Furthermore, the high-resolution TEM images of the C zone commonly show lattice images of bundles of crystallites with thicknesses, a slightly curved or linear morphology, numerous edge dislocations, and low-angle junctions to each other similar to those observed for glauconite grains by Ireland *et al.* (1983), Amouric and Parron (1985), and Vali and Köster (1986). These features of the lattice images, with their loss over relatively small distances, also attest to a relatively poor crystalline order consistent with the presence of glauconitic minerals.

The presence of A zones throughout vermicular glaucony could be explained by the observation that some A zones appear to have undergone a separation or splaying process (Figure 7). The growth of zone B minerals where A zones are splayed could continue far enough along the basal cleavage of the parent zone to part several thinner A zones from their thicker parent. That A zones can be found throughout the vermicular



Figure 13. Photomicrograph of biotite flake fanned at its edges (direction of fanning is indicated) by the growth of a green randomly microcrystalline mineral(s) between splayed biotite sheets. Thicker biotite zones are apparent in the center of the flake (vertical arrow).

glaucony grains suggests that, if they do represent parted remnants of a higher order mica flake, then the A zones can remain chemically and physically stable once they have been cleaved from the initial phyllosilicate flake. It also suggests that their chemical components are not required for the bulk of glauconitic mineral growth in zones B and C. Neither of these interpretations support the mechanism of layer-by-layer transformation of mica substrates by glauconite to form vermicular glaucony.

At the finer scale of lattice images, however, the prising of small amounts of A zone mineral lattices into the B zone (Figure 6) suggests some degree of interaction between the minerals of these two zones. This interaction involves at least a physical degradation of the lattices cleaved from the A zone parent, as evidenced by the less strongly linear and less well-defined lattice images compared with those of their parent A zone. Whether such lattices remain inert within the B zone or whether they undergo further chemical or physical modification remains unclear at this time.

The variation in thickness of B and C zones in a direction perpendicular to the elongation direction (Figure 3) suggests that they cannot be treated as planar features extending through the vermicular glaucony grain. Conversely, A zones, despite some splaying and undulation, are more uniform in thickness and have more strongly linear orientations. This suggests that they exist as broadly planar features. Thus, the prominent cleavage of vermicular glaucony, oriented at right angles to the elongation direction, appears to owe its origin to the presence of the A zone minerals.

The recognition of three zones in TEM images could be the result of sectioning the type of three-dimensional images displayed in the accordion-like grains of Odin (1988, Figure 7, p. 259). In that case glauconitic minerals were shown to develop on micaceous substrates firstly in a "box-work" and then a "rosette" fabric.

In summary, the sharp line between zone A and zones B and C is interpreted as representing a genetic change. Zones B and C show no such physical boundary and are likely to be genetically linked. Zone A minerals are interpreted to have formed at the higher pressures and temperatures of metamorphic or igneous environments, and those of zones B and C are interpreted to comprise predominantly glauconitic minerals formed in the marine environment.

Evolution of zonation in vermicular glaucony

If the above interpretations of the identity of the three zones are correct, then the following is a possible scenario describing the evolution of alternating A, B, and C zones in vermicular glaucony grains. The initial sites for glauconitic mineral nucleation may be provided by frayed mica edges or partings developed during weathering and transportation. Such partings could be developed anywhere along the micaceous sheets,

but are presumably more likely to have been initiated at the edges (Figure 13). Glauconitic minerals of zone B, growing on the surfaces of zone A minerals, appear to be the initial growth phase. This is evident from the observation of some areas in which zone B only is present between micaceous sheets (Figure 7). Furthermore, where zone C occurs, it is always surrounded by a variously developed B zone (Figures 3–5). Thus, the B zone is always the closest zone to what is interpreted as the detritally derived A zone.

The subparallel orientation of growth in zone B appears to be controlled by the confining effect of the immediately adjacent zone A mineral. This is particularly evident where splayed or curved A zones exhibit similarly oriented bundles in B zones (Figure 7). It is also possible that the presence of some A zone fragments within the B zone may control glauconitic mineral development. The period of time during which confined growth occurs could also be influenced by growth of other B and C zones, at different rates and in opposing directions, elsewhere in the expanding vermicular grain. This idea offers another possibility of a control on the development of the three zones and vermicular glaucy morphology: that of post-growth or syn-growth modification of the morphologies of A, B, and C zones due to processes such as the accommodation of stress created by glauconitic mineral growth.

The A zones are of different thickness throughout the vermicular glaucy grains, probably recording different susceptibility to cleavage within the initial micaceous substrate. This susceptibility was presumably due to crystallographic or mineralogical imperfections, either inherent in the mineral or induced by the presence of other minerals formed during weathering at outcrop and abrasion during transportation.

Once formed, the growth of zone B-oriented minerals appears to prise open the phyllosilicate sheets (Figure 7). New growth sites are created as glauconitic minerals of zone B further infiltrate along the micaceous cleavage of zone A. At some point as the phyllosilicate layers move apart, glaucy growth becomes less and less confined with development of more randomly oriented and circular bundles of zone C.

Less well-confined glauconitic mineral growth may occur earlier in some areas in the phyllosilicate flake than others, whereupon the B zone would presumably be thinner and more poorly developed while the C zone would be thicker because it was able to develop longer into relatively unrestricted space. Conversely, thick B zones with no C zone development suggest longer periods of confinement. The formation of the C zone bundles in areas where growth has hitherto been restricted by confinement would further push adjacent A zones apart. This would continue to expand and thicken the original phyllosilicate flake in a direction broadly perpendicular to the platy micaceous cleavage.

The amount of expansion, measured as the thicknesses of B and C zones compared with that of their surrounding A zones, must be orders of magnitude greater than the initial thickness of the phyllosilicate flake.

CONCLUSION

Vermicular glaucy grains comprise alternating zones of minerals with different morphologies. The morphologies of vermicular glaucy in zones B and C are similar to those documented for nonvermicular glauconite grains. However, there is some indication that some modified A zone minerals are present in the B zone. The morphology of zone A is unlike that documented for glauconite, but is similar to that of phyllosilicates with higher structural order, such as biotite and muscovite. Future work should concentrate on documenting any chemical or crystallographic differences that may occur between the three zones so as to clarify the interpretations based morphology.

If the interpretations based on morphologies of the three zones are correct, then the neoformation mode of origin for vermicular glaucy is largely supported by this study. For example, the presence of A zone minerals throughout vermicular glaucy grains suggests their components are not necessarily required for glaucy, as would be the case if a simple transformation process was involved. However, the observation of lattice-fringe images at the contact of the A and B zones, cleaved off parent A zones, suggests at least physical modification of the A zone mineral(s). It is possible this also involves some chemical modification that could allow an avenue for application of the transformation theory.

The fact that Tapper and Fanning (1968) did not find diffraction maxima attributable to biotite or muscovite or indeed any other phyllosilicate of suitably high structural order could be the result of two factors. 1) The grains analyzed in this study and those examined by Tapper and Fanning are different types of vermicular glaucy, with different origins, but which apparently lead to a similar end point. 2) The amount of the original higher order micas such as biotite or muscovite remaining in vermicular glaucy is either a) low enough to be beyond intrinsic detection limitations of X-ray powder diffraction or b) low and variable enough not to be picked up by examining a small number of grains.

ACKNOWLEDGMENTS

The author is grateful for instruction on the preparation for, and use of, ion-beam thinning equipment by Dr. J. Palmara and Dr. P. Phakey of the Monash University, Melbourne, Australia. Dr. Palmara thinned a further set of samples at a later date. Mr. A. Mitchell in the Otago Medical School provided instruction in the operation of the TEM. Mr. J. Pillidge constructed the initial thin sections required for ion-beam

thinning. Drs. J. J. Aitken, C. A. Landis, and A. Reay provided discussion and critical comment. This study represents part of a doctorate thesis completed at the University of Otago.

REFERENCES

- Amouric, M. and Parron, C. (1985) Structure and growth mechanism of glauconite as seen by high-resolution transmission electron microscopy: *Clays & Clay Minerals* **33**, 473–482.
- Banfield, J. F. and Eggleton, R. A. (1988) Transmission electron microscope study of biotite weathering: *Clays & Clay Minerals* **36**, 47–60.
- Brown, E. H. (1963) The geology of the Mt. Stoker area, Eastern Otago. Part 1. Metamorphic geology: *N. Z. J. Geol. Geophys.* **6**, 847–871.
- Burst, J. F. (1958a) "Glauconite" pellets: Their mineral nature and applications to stratigraphic interpretations: *Bull. Am. Assoc. Petrol. Geol.* **42**, 310–327.
- Burst, J. F. (1958b) Mineral heterogeneity in "glauconite" pellets: *Amer. Mineral.* **43**, 481–497.
- Carter, R. M. and Norris, R. J. (1976) Cainozoic history of southern New Zealand: An accord between geological observations and plate-tectonic predictions: *Earth Planet. Sci. Lett.* **31**, 85–94.
- Carter, R. M. (1988) Post-breakup stratigraphy (Kaikoura Synthem: Cretaceous–Cenozoic) of the continental margin of southeastern New Zealand: *N. Z. J. Geol. Geophys.* **31**, 405–429.
- Gallagher, E. W. (1935) Geology of glauconite: *Bull. Am. Assoc. Petrol. Geol.* **19**, 1569–1601.
- Iijima, S. and Buseck, P. R. (1978) Experimental study of disordered mica structures by high resolution electron microscopy: *Acta Cryst.* **A34**, 709–719.
- Ireland, B. J., Curtis, C. D., and Whiteman, J. A. (1983) Compositional variation within some glauconites and illites and implications for their stability and origins: *Sedimentology* **30**, 769–786.
- Lee, J. H., Ahn, J. H., and Peacor, D. R. (1985) Textures in layered silicates: Progressive changes through diagenesis and low-temperature metamorphism: *J. Sedim. Petrol.* **55**, 532–540.
- McMillan, S. G. (1993) The Abbotsford Formation: Ph.D. thesis, University of Otago, Dunedin, New Zealand, 646 pp.
- Norris, R. J., Carter, R. M., and Turnbull, I. M. (1978) Cainozoic sedimentation in basins adjacent to a major continental transform boundary in southern New Zealand: *J. Geol. Soc. Lond.* **135**, 191–205.
- Odin, G. S. (1972) Observations nouvelles sur la structure de la glauconie en accordeon: Description du processus de genèse par néoformation: *Sedimentology* **19**, 285–294.
- Odin, G. S., ed. (1988) Green marine clays: *Developments in Sedimentology* **45**, Amsterdam. Elsevier, 445 pp.
- Odin, G. S. and Matter, A. (1981) De glauconiarum origine: *Sedimentology* **28**, 611–641.
- Page, R. H. (1980) Partial interlayers in phyllosilicates studied by transmission electron microscopy: *Contrib. Mineral. Petrol.* **75**, 309–314.
- Phakey, P. P., Curtis, C. D., and Oertel, G. (1972) Transmission electron microscopy of fine-grained phyllosilicates in ultra-thin rock sections: *Clays & Clay Minerals* **20**, 193–197.
- Tapper, M. and Fanning, D. S. (1968) Glauconite pellets: Similar X-ray patterns from individual pellets of lobate and vermiform morphology: *Clays & Clay Minerals* **16**, 275–283.
- Vali, H. and Köster, H. M. (1986) Expanding behaviour, structural disorder, regular and random irregular interstratification of 2:1 layer silicates studied by high resolution images of transmission electron microscopy: *Clay Miner.* **21**, 827–859.
- Wood, B. L. (1968) Otago Schist: in *Geological Map of the Dunedin District. 1:50,000*, W. N. Benson, ed., New Zealand Geological Survey Miscellaneous Series Map 1, Department of Scientific and Industrial Research, Wellington, New Zealand.

(Received 27 April 1992; accepted 1 September 1993; Ms. 2218)